A Novel Modular Tonometry-Based Device to Measure Pulse Pressure Waveforms in Radial Artery

Article *in* Journal of Medical Devices · January 2018

DOI: 10.1115/1.4039010

CITATIONS
2

READS
338

7 authors, including:

Mohammad Ikbal Choudhury
Johns Hopkins University
15 PUBLICATIONS **57** CITATIONS
SEE PROFILE

K K Deepak
All India Institute of Medical Sciences, New Delhi India
114 PUBLICATIONS **1,304** CITATIONS
SEE PROFILE

Anamika Prasad
South Dakota State University
28 PUBLICATIONS **145** CITATIONS
SEE PROFILE

Sitikantha Roy
Indian Institute of Technology Delhi
35 PUBLICATIONS **224** CITATIONS
SEE PROFILE

Mohammad Ikbal Choudhury
Department of Applied Mechanics,
Indian Institute of Technology Delhi,
Block 4, Academic Building,
New Delhi 110016, India
e-mail: ikbal.choudhury.nits@gmail.com

Pranjal Singh
Department of Applied Mechanics,
Indian Institute of Technology Delhi,
Block 4, Academic Building,
New Delhi 110016, India
e-mail: pranjalnewton@gmail.com

Rajneesh Juneja
Department of Cardiology,
All India Institute of Medical Science,
Neurosurgery and Cardiac Surgery Building,
New Delhi 110016, India
e-mail: rjuneja2@gmail.com

Suneet Tuli
Center for Applied Research in Electronics,
Indian Institute of Technology Delhi,
Block 3, Academic Building,
New Delhi 110016, India
e-mail: suneet@care.iitd.ac.in

K. K. Deepak
Department of Physiology,
All India Institute of Medical Science,
New Delhi 110016, India
e-mail: kkdeepak@gmail.com

Anamika Prasad[1,2]
Mechanical Engineering Department,
South Dakota State University,
Brookings, SD 57007
e-mail: Anamika.Prasad@sdstate.edu

Sitikantha Roy[1]
Department of Applied Mechanics,
Indian Institute of Technology Delhi,
Block 4, Academic Building,
New Delhi 110016, India
e-mail: sroy@am.iitd.ac

A Novel Modular Tonometry-Based Device to Measure Pulse Pressure Waveforms in Radial Artery

The paper presents the development of a new device for measuring continuous pulse pressure waveforms (PPW) from the radial artery via applanation tonometry. The development focuses on improved accuracy, open and affordable design using off-the-shelf components, and greater user control in setting operational and calibration parameters to address user variability. The device design parameters are optimized through a tissue device interaction study based on a computational model. The design incorporates modular components and includes a sensor module for arterial flattening and pressure pick-up, a differential screw mechanism and a related algorithm for controlled stepwise motion and data collection during flattening, and a brace for wrist-flexion adjustment. Maximum pulse amplitude (PA) was used as an indicator of the optimum level of arterial flattening for recording the PPW. The PPW was observed to distort due to changes in parameters like gel-head placement, hold-down pressure (HDP), and wrist extension. The pressure waveforms collected using the device were validated using limited data against established products and showed good correlation within ±1.96 standard deviation of the mean difference in a Bland–Altman plot. This paper thus details the development of a simple and validated mechanical design to measure PPW using arterial tonometry. [DOI: 10.1115/1.4039010]

1 Introduction

Arterial pulse has been an essential source of information in the prognosis and diagnosis of a variety of health conditions. The systemic study of pressure pulse waveform (PPW) using engineering tools dates back to 1855 when Vierordt developed a pulse waveform scanner [1]. PPW has been found to have useful information regarding the overall cardiovascular health of a person. For example, an increase in pulse pressure is indicative of stiffening of conduit vessels [2,3]. Radial PPW converted to aortic pressure waveform via a suitable transfer function is indicative of a number of cardiac health conditions [4–7]. Analysis of pressure waveforms in time domain provides information on aging and other factors [6,8]. Using Fourier transform to study radial artery waveforms in frequency domain provides information about factors affected by the mechanical resonance between the heart and other organs [9]. Other similar studies are a further indication of a connection between pathological change in various organs and its effect on the harmonic parameters of pressure waveforms [10,11].

It is therefore evident that the focus is gradually shifting from discreet two-value blood pressure (BP) readings to a pressure waveforms-based analysis of the health of cardiovascular systems and other organs [12]. Applanation tonometry has proven to be a "gold standard" for measuring high-fidelity pressure waveforms due to its simplicity and its noninvasive, tactile nature of measurement [12,13]. In this method, the artery is partially flattened to an extent where the external force balances the internal aortic BP

[1]A. Prasad and S. Roy equally contributed to this work.
[2]Corresponding author.
Manuscript received February 10, 2017; final manuscript received December 14, 2017; published online January 31, 2018. Editor: William Durfee.

leading to maximum arterial compliance, and BP is recorded by a sensor placed on the flat section of the artery.

Many tonometry-based devices currently exist for measurement of PPW and BP [14,15]. The focus of most devices and related studies has been divided between sensor fabrication and systems integration for ambulatory and clinical measurement. From a sensor design perspective, Lee et al. [16] developed a cantilever array-based tactile sensor by silicone bulk-micromachining. Kim et al. [17] developed an arterial tonometer sensor array using piezoresistive sensor elements and polydimethylsiloxane coating. Shioya and Dohi [18] reported the development of a microtriaxial force sensor consisting of two pressure sensor elements and six shear stress sensor elements.

From the system integration and device design perspective, important parameters include the sensor housing design, sensor-centering mechanism over the artery, hold-down pressure (HDP) for arterial flattening, and the angle of wrist extension during measurement. The sensor housing holds the sensor and is typically used to flatten the artery. In the process of arterial compression, the housing design can create additional stresses on the surface leading to errors in reading [19]. Sensor centering over the artery is achieved by either manual location for maximum palpations or manual location combined with automatic feedback algorithms for improved sensitivity [20]. HDP affects pulse amplitude (PA) and contours of pressure waveform [21–23]. Most existing devices apply the desired HDP through a feedback mechanism via simultaneous reading from brachial artery cuff [6]. Proprietary algorithms are used for setting the desired HDP and for waveform corrections and calibrations. Finally, wrist flexion causes the radial artery to become superficial, and, hence, it is easier to detect PPW. Many commercial devices come with an attached stiff brace for setting a desired angle of flexion.

From the device design and integration point of view, almost all current commercial devices are closed systems with automatic and propriety methods for selection of operation parameters (selection of HDP, amount of wrist flexion, sensor calibration). Device parameters such as the amount of wrist flexion and the selection of HDP mostly remain similar across different patient groups. Devices in some cases become bulky due to the incorporation of pneumatic chambers [19] and/or stepper motors [20] for automatic centering. Finally, most devices are expensive, which limits their availability in low- and medium-income countries. Low- and medium-income countries account for 80% of cardiovascular death [24]. In such scenarios, large-scale use of cardiovascular health monitoring devices can play an important role in understanding cardiovascular disease and identifying early risk factors across patient groups.

In light of these observations, in this work, we address the aspects of design factors as well as a global need for a new tonometry-based device. The developed device focuses on improved accuracy and analysis, open and affordable design using off-the-shelf components, and greater user control in setting operational and calibration parameters to address user variability. Specifically, we describe (a) a novel sensor module that works with an off-the-shelf tactile-based force sensor; (b) data collection protocol to measure PPW with high-fidelity and greater control; and (c) an underlying computational simulation of device–tissue interaction, which guides the sensor module design and data collection protocol.

2 Device Development

The overall device and its placement, shown in Fig. 1(*a*), consist of the main unit and a wrist flexion mechanism. The main unit, shown schematically in Fig. 1(*b*), consists of three main parts: (1) a differential screw, (2) a device enclosure, and (3) a sensor module. The differential screw applies precise and sequential HDP for arterial flattening. The device enclosure holds the differential screw and sensor module in place. The sensor module, in turn, houses the sensor and related components for uniform pressure application over the sensing area. The sensor module, shown schematically in Fig. 1(*c*), consists of (a) a snap-fit base plate connected to the differential screw, (b) a tactile-based force sensor, (c) a spring element or gel layer, (d) an arterial rider or gel head, and (e) top cover. The elements of the sensor module and their function are described in detail in Sec. 2.2.

Overall, the device was designed to control three operational parameters known to affect tonometry readings, namely (a) placement of the sensor, (b) HDP, and (c) angle of wrist extension. Placement of the sensor and centering of the device on top of the radial artery is controlled manually using a finger palpation technique. The differential screw mechanism and underlying algorithms control HDP. Ideally, pressure waveforms are said to be noted when pulse amplitude is maximum, which is known to occur at high percentage flattening of the artery [23]. Mechanically achieving and maintaining optimal arterial flattening by simply tightening the brace or using a one-size-fits-all plunger pressure across different user groups can be erroneous. Here, the differential screw mechanism with an effective pitch of 0.5 mm enables manual control in arterial flattening with precise upward

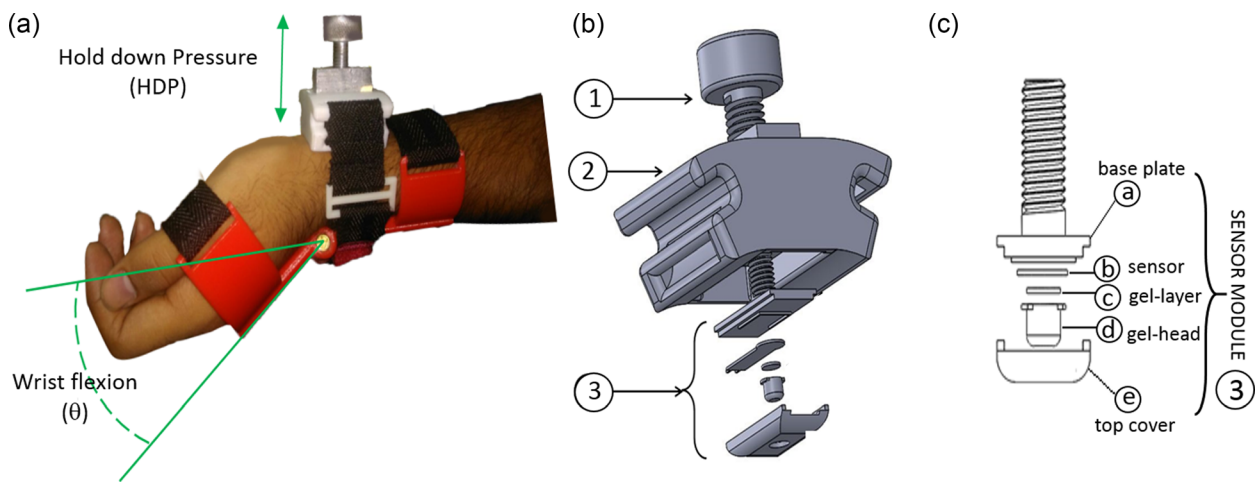

Fig. 1 (*a*) The device is placed on the wrist showing the main unit and the flex-lock brace, (*b*) details of the main unit and its components, and (*c*) details of the sensor module and its components. The main device consists of (1) differential screw, (2) device enclosure, and (3) a sensor module. The sensor module consists of (*a*) base plate, (*b*) tactile sensor, (*c*) gel layer, (*d*) gel head, and (*e*) top cover. The flex-lock brace is used to control and fix the angle of wrist flexion θ, and differential screw is used to sequentially apply and control the HDP for arterial flattening.

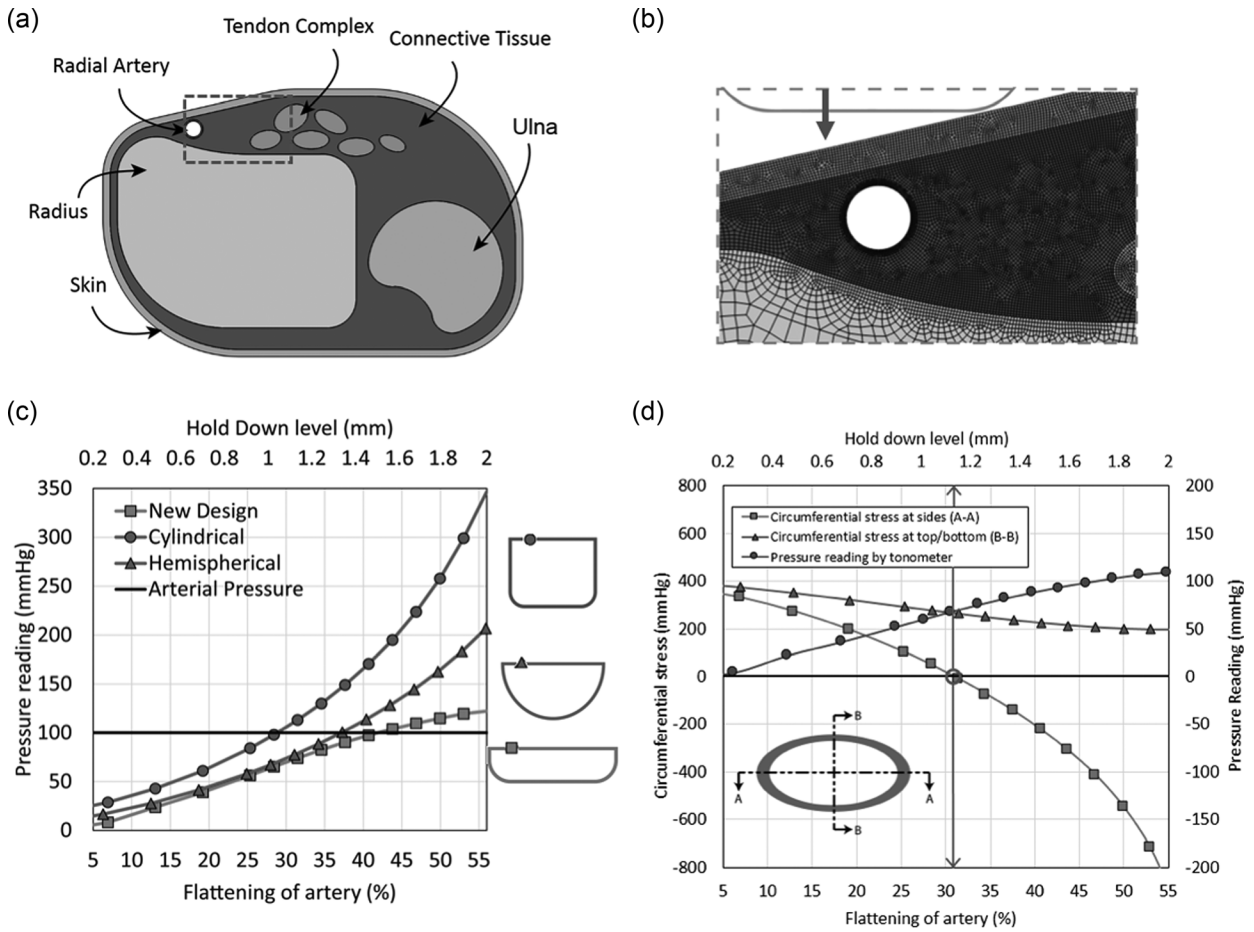

Fig. 2 Computational analysis for sensor design, showing (*a*) idealized model of human wrist, (*b*) meshed computational domain near the aorta showing placement of tonometer plunger, (*c*) plot showing average contact pressure versus arterial flattening for three tonometer geometries, and (*d*) plot showing circumferential stress variation in artery wall versus applied hold down level during tonometry. Details of the simulation and materials parameters are provided elsewhere [25].

and downward movement in submillimeter steps. The underlying algorithm provides an indicator for user-specific selection of an optimal flattening level for obtaining maximum pulse amplitude. Finally, the angle of wrist extension is controlled via the flex-lock brace, shown in Fig. 1(*a*), which allows the user to select the angle of wrist flexion and locks and maintains the selected angle throughout the measurement.

2.1 Sensor Module. Figure 1(*c*) shows a detailed view of the sensor module and its components, comprising of (a) a base plate, (b) pressure sensor, (c) gel layer, (d) gel head, and (e) top cover. The base plate provides a hard and flat surface for the sensor on one side and the differential screw on the other. Thus, turning the differential screw allows the sensor module to move uniformly down, keeping the sensor surface flat at all times. The gel layer placed between the sensor and the gel head acts as an elastic spring for force transfer to the sensor and is made of a uniform circular plate of thickness 0.5 mm and diameter 5 mm. The diameter was selected to be comparable to the diameter of the active area of the sensor. The gel head, in contact with the gel layer at one end and user skin on the other, is designed as a tapered cylinder with a diameter of 5 mm at the end in contact with the gel layer and 2 mm at the end in contact with the skin. The diameters of 5 mm and 2 mm were chosen to match the active area of the sensor on one end and the diameter of the radial artery on the other. With this design, when the gel head is centered correctly at the radial artery, it essentially rides the artery to faithfully transfer pulse pressure forces to the sensor via the attached gel layer, which in turn distributes the pressure uniformly over the sensor active area. Thus, the gel head and gel layer essentially act as a spring–mass system to capture PPW. Due to a smaller area of pressure pick-up, centering of gel head on the artery is important. Results from centering errors are discussed in Sec. 4.3.

All components above, except the sensor, were 3D printed. The base plate, top plate, and gel head were made of hard thermoplastic (acrylonitrile butadiene styrene or ABS), and the gel layer was made of room-temperature vulcanizing silicone elastomer (Dow Corning, Auburn, MI) with Shore A hardness of 30.

A computational simulation of a human wrist section was chosen to guide and optimize the design of the plunger (the top cover of the sensor module). Figure 2(*a*) shows the details considered in the computational model. Figure 2(*b*) shows the meshed domain near the location of the artery. The simulation described in detail elsewhere [25] incorporates hyperelastic tissue properties of skins and aorta and the frictional interaction between the device and skin. Parametric variations in material and geometric parameters were considered to account for the effect of patient variability on device performance. Three plunger geometries were chosen for analysis, two of which (hemispherical and cylindrical) were chosen to match plunger geometry in commonly used tonometry devices. The third (flat plunger), the new geometry, was incorporated in the device as the top cover of the sensor module. Results showed the flat plunger was less sensitive to sensor placement, was not influenced by edge contact stresses, and was minimally influenced by patient-specific variability [25]. Further, as shown in Fig. 2(*c*), the flat plunger demonstrated a linear trend in recorded pressure with increasing HDP, unlike the nonlinear trend

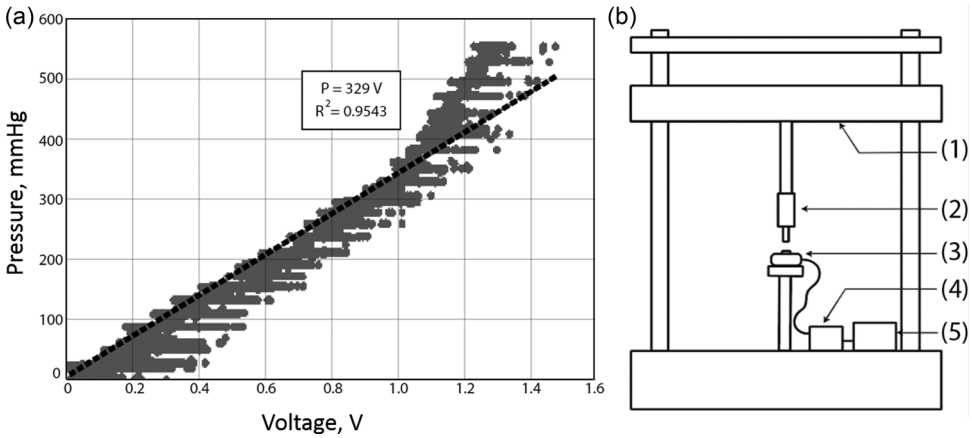

Fig. 3 (*a*) Sensor calibration plot showing applied pressure versus voltage relationship and (*b*) schematic of experimental setup of sensor calibration where universal testing machine or UTM (1) with a load cell (2), was used to apply pressure on the sensor module (3), and pressure–voltage data captured and recorded via electronic circuit (4) and NI (National Instruments) data acquisition card (5)

for the other two designs. Finally, we observed that tonometry loading resulted in directional loading–unloading of the aortic wall as shown in Fig. 2(*d*). As discussed in Sec. 3.1, the observed directional loading concept forms the basis of selection of optimum hold-down level for PPW measurement.

2.2 Sensor Selection and Calibration. We selected an off-the-shelf tactile force sensitive resistor (Interlink Electronics, Westlake Village, CA) for its reported sensitivity, reproducibility, robustness, and low hysteresis [26]. The selected sensor active area of diameter of 5 mm was almost twice that of a typical radial artery diameter of 2.6 ± 0.2 mm [25]. Hence, as detailed earlier, the sensor module design incorporated a tapered gel-head and a constant thickness gel layer for uniform pressure distribution from the smaller pick-up area of the radial artery to the larger active area of the sensor.

The pressure–voltage calibration curve (Fig. 3(*a*)) was obtained by using a Universal Testing Machine (Fig. 3(*b*), schematic of the experimental setup) with a 50 N load cell (Dak systems, Mumbai, India), and a DAQ card (National Instruments, Austin, TX), with a data acquisition rate set at 1000 samples per second. The pressure (P)–Voltage (V) calibration relationship $P = 329*V$ ($R^2 = 0.95$) was obtained by fitting a linear function to the calibration plot for the pressure range from 0 to 400 mm Hg.

As the sensor module compresses the skin, the contact stresses on edges of the sensor module increase due to wrist curvature and interaction with stiffer tendons. These stresses are difficult to predict and can lead to error in sensor readings. In the current design, the pressure pick-up area (i.e., gel-head) is located at the center of the plunger, away from the area of high contact stresses at the edges, thus avoiding the edge-effect errors.

3 Principles and Parameters for Device Usage

3.1 Protocol for Selection of Hold-Down Level for Pulse Pressure Waveforms Selection. The artery wall under in situ conditions is prestressed due to the presence of blood pressure. During an oscillometric cuff-based measurement, external cuff pressure is applied uniformly across the arm section to balance the internal blood pressure. At the point where externally applied pressure balances mean arterial pressure, the arterial wall experiences complete unloading [27]. However, in the case of tonometry, the artery is compressed increasingly and predominantly in the direction of hold down. During various stages of arterial compression, it has been reported that pulse amplitude first increases, reaches a maximum, and then decreases as the hold-down pressure is increased [21–23]. Hence, a suitable and consistent value of compression level needs to be selected for recording the right PPW during tonometry.

As shown in Fig. 2(*d*) and discussed in detail elsewhere [25], it was shown that the artery wall "unloads" (i.e., circumferential stress reduces) faster at the sides in direction of hold down (along section A-A′, Fig. 2(*d*)) than at the top and bottom (along section B-B′, Fig. 2(*d*)). Specifically, for the analysis presented in Fig. 2, circumferential stress at Section A-A reduced to zero at 33% of arterial compression, while at the same level of compression, circumferential stresses at Section B-B′ remained nonzero. This complete loss of artery wall compliance on the sides at 33% level of compression is expected to result in maximum palpitation and, hence, in maximum pressure pulse amplitude transfer to the surface. Hence, the point of maximum pulsation, consistent with complete arterial unloading at the sides, is taken as a criterion for the selection of PPW in our protocol.

3.2 Protocol for Data Acquisition. The device was used to acquire PPW from five healthy male subjects in the age group of 20–25 years. The study was conducted by taking informed consent from all the volunteers. The data acquisition protocol was similar to that used for BP monitoring via cuff-based devices (i.e., sitting position with both wrists placed at the same level). For each case, measurements were taken consistently at the same time of the day. The device was placed to position the gel head at the geometric center of the artery. The sensitivity of the data to gel-head centering is discussed in Sec. 4.3.

During the same sitting, data were also acquired using a standard mercury Sphygmomanometer (Supreme Surgico, New Delhi, India) at the brachial artery, and Collins tonometer (Colin Corporation, Komaki, Japan) at the radial artery. Since the new device and the Collins tonometer each take measurements from the radial artery, it was not possible to take simultaneous readings from the same artery. Hence, for simultaneous PPW recording, the new device was placed on the left radial artery, and Collins tonometer (CT) was placed on the right. This step was repeated after interchanging their respective positions. BP values from both arms were also measured using the sphygmomanometer to check for possible errors. The sphygmomanometer reading was used to calibrate PPW to BP as in most commercial tonometry devices, and the Collins tonometer was used for waveform comparison.

Pressure pulse waveform was captured at varying levels of arterial flattening using the differential screw mechanism. Essentially, PPW was recorded in several steps by gradual loading (compressing) of the artery via downward motion of the

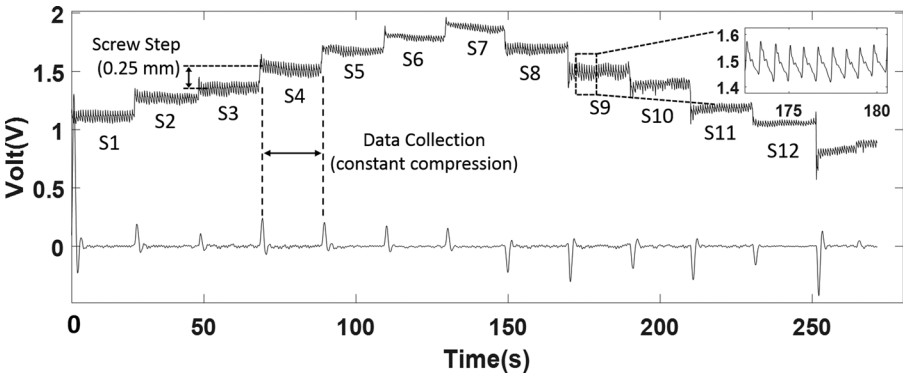

Fig. 4 Plot showing voltage versus time data during complete arterial loading (S1 to S7) and unloading (S8 to S12) steps. The top plot comes from the static voltage component (due to mean BP and hold down pressure) and fluctuating voltage component (pulse pressure variation). The bottom plot corresponds to the data after filtering of the static component, thus showing only the fluctuating component (pulse pressure changes) having a mean of zero for each step.

differential screw in submillimeter steps up to the point of maximum PA. Similarly, PPW was also collected during gradual unloading (uncompressing) of the artery via upward motion of the differential screw in submillimeter steps. From the complete step of loading–unloading PPW thus collected, the right PPW was identified using an in-house algorithm.

Figure 4 shows complete PPW data for a particular case of loading–unloading protocol. Each step corresponds to one screw rotation of 180 deg, which makes the sensor module move downward (here S1 to S7) or upward (here S8 to S12) by 0.25 mm. At each rotation step, data were collected for a period of 10 to 20 s before loading or unloading to the next step. The sensor analog signals were digitized using connected NI DAQ card (National Instruments, Austin, TX) with a sampling rate of 33 samples per second. Finally, the data were sent via a connected personal computer for visual feedback, storage, and postprocessing.

3.3 Post Processing. The voltage recorded by the sensor feeds from a combination of sources. Essentially, blood pressure in the artery contributes to a static component (static-I due to mean BP) and a fluctuating component of the voltage reading. In addition, HDP applied to the sensor for compression of skin and artery via the differential screw mechanism leads to additional static pressure (static-II). Thus, the top line in Fig. 4 shows the total voltage and corresponds to data from static-I + static-II+ fluctuating component. During postprocessing, the raw signal was filtered by using a band pass filter with a cut-off of 0.05 Hz to remove all static components (Static I + static-II), thus resulting in only the fluctuating voltage about a mean of zero. The filtered signal is shown at the bottom plot of the figure. To calculate the BP from the filtered signal, it is first necessary to identify the right step (based on maximum pulse amplitude) in loading and unloading cycles, and then scale the selected step from a mean of zero to a precalculated mean arterial pressure (P_{MAP}) obtained separately using the sphygmomanometer. As needed, the recorded voltage was converted to pressure using the linear pressure–voltage calibration equation.

4 Results and Discussion

4.1 Pulse Amplitude. Figure 5(*a*) shows a Bland–Altman plot to demonstrate the statistical agreement between PA recorded from five subjects using the new device and the sphygmomanometer. All readings from the new device were taken while maintaining a constant angle of wrist extension (θ) of 40 deg. All data points lie within ± 1.96 standard deviation of the mean difference. Due to small sample size, the 95% confidence interval (CI) of the limits of agreement (± 1.96 standard deviation lines) is large. Therefore, the probability that the maximum clinically allowed difference may lie within 95% CI interval also increases. However, increasing the number of subjects at different ages, genders and health conditions would decrease the 95% CI interval margin. The PA was observed to be somewhat higher in the sphygmomanometer than the tonometry data, which is expected due to pulse amplitude amplification effects at the brachial artery.

4.2 Pulse Waveform. There are two main methods for pulse waveform analysis, namely, point-based method and area-based method [7]. Point-based analysis is used to determine various risk factors using indices that are ratios of the lengths of specific points on the waveform in time domain. Stiffness index and pulse wave velocity are well-known factors in this category [28]. Area-based analysis is used in blood volume monitoring like the cardiac output. Here, we used the point-based methods to compare waveforms obtained by the new device versus the Collins tonometer. As marked in Fig. 5(*b*), radial artery waveforms are characterized via the crest time ($T1$), dicrotic wave time ($T2$), total pulse duration time (TPT), systolic amplitude (A1), and dicrotic amplitude (A2). The term $\Delta T = (T1–T2)$ is known to have a direct correlation with the stiffness index of the artery [27]. The value of TPT is used to calculate important indices such as the ejection duration and diastolic time interval. Here, we compared ΔT and TPT values for the five subjects recorded by two devices. The results are shown in Fig. 5(*c*) for ΔT and Fig. 5(*d*) for TPT. For all five subjects, the values were found to be close, with an average difference in ΔT being 2.1% and that of TPT being 4.2%, respectively.

4.3 Effect of Centering. To capture PPW accurately in tonometry, the sensing element must be placed on the geometric center of the radial artery. An off-center placement of the sensor may result in distorted waveforms and an error in PA. Earlier computational analysis showed that when the device is centered at the radial artery, PA was fairly uniform over the range of ± 1r (r = radius of the artery) from the center, and gradually reduced away from the center [25]. Hence, the current device is expected to be less sensitive to small errors in centering. This is validated here by measuring waveforms from five subjects by placement of gel head at various positions from the center.

As discussed earlier, the gel head was placed at the geometric center of the artery by manually identifying the location using finger palpation. Sensitivity of the data due to a change from the ideal centered position was analyzed by placing the sensor module at three different locations on the radial artery of the left hand.

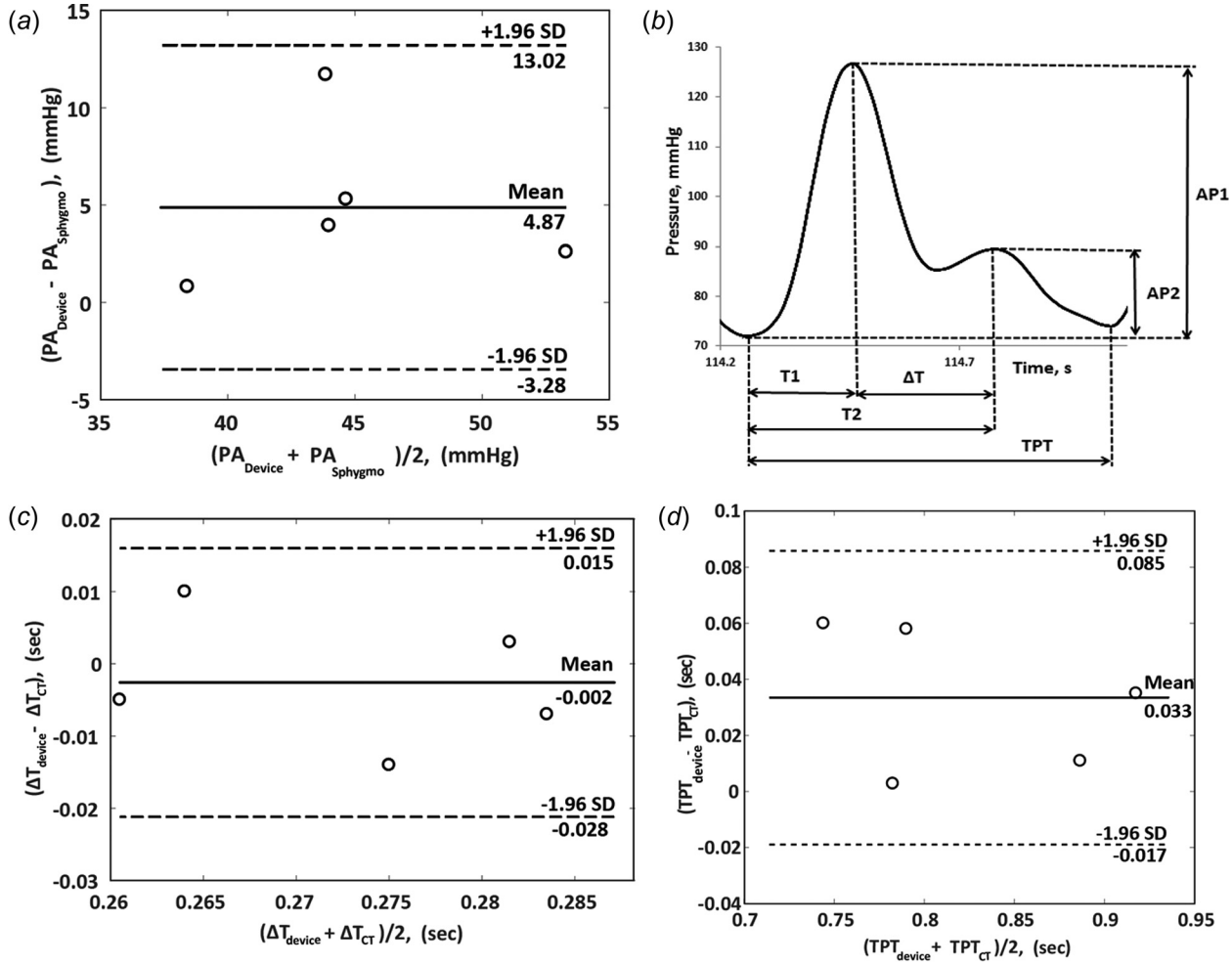

Fig. 5 (*a*) Bland–Altman plot of PA measured using a sphygmomanometer and the new device. (*b*) Typical pulse waveform in time domain with the key points of the waveform marked namely crest time (*T*1), dicrotic wave time (*T*2), TPT, Systolic amplitude (A1), and dicrotic wave amplitude (A2), (*c*) Bland–Altman plot of $\Delta T = T2 - T1$ measured from the new device and CT, and (*d*) Bland–Altman plot of TPT values measured from the new device and CT. Data were recorded for five different subjects using the protocol defined. On all the Bland–Altman plots, ±1.96 SD and 95% CI lines are also marked. The CI line is fairly large due to limited subject cases, and is expected to decrease with increasing subject number and subject variability (gender, age group, health conditions).

The values $x = -1$ mm, 0 mm, and 1 mm correspond, respectively, to the left, center, and right of the artery. All readings were taken while maintaining a constant angle of wrist extension ($\theta = 40$ deg) using the flex-lock brace. As expected and shown in Fig. 6(*a*), average PA for all subjects was found to be maximum when the sensor was placed exactly at the center as compared to the positions 1 mm to the left or right of the artery. This indicates that the pressure transmission is highest when the artery is right below the

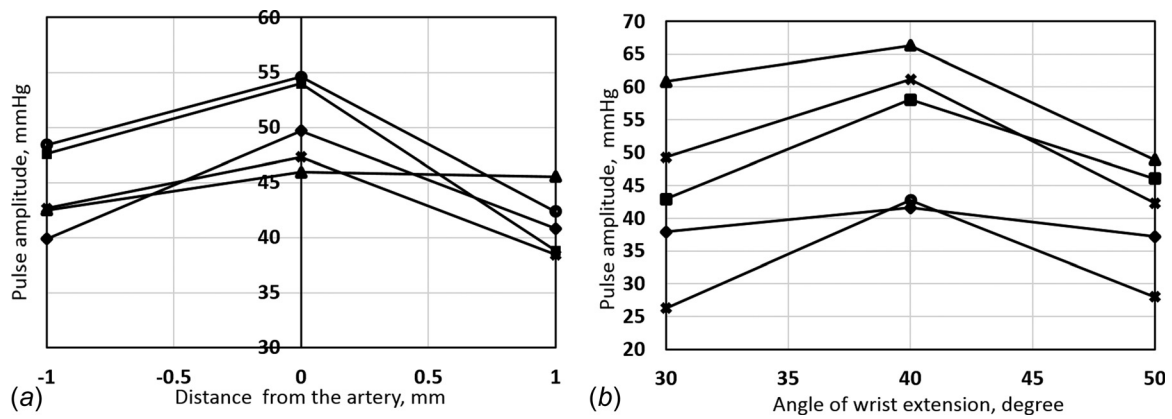

Fig. 6 (*a*) Variation of PA with shifting of a module over and away from the artery and (*b*) variation of PA with the angle of wrist extension (θ) where the markers indicate different subjects

gel head. Since the pattern is repeatable across all patients measured here, a suitable feedback algorithm can be incorporated to correct for small centering errors.

Interestingly, as shown in Fig. 7, the shape of PPW was also observed to change due to arterial centering. It was observed that the dicrotic notch dips along the pressure axis when the gel head is displaced by 1 mm on both sides of the artery. This can be attributed to the nonuniform flattening of the artery when the location of gel head has an offset. The radius has a slope and artery might also slip away if the compression is nonuniform. These factors may cause the gel head to lose contact with the skin and hence result in the observed irregular waveforms.

4.4 Effect of Wrist Extension. A change in the angle (θ) of wrist extension can cause the artery to shift in the vertical direction. As a result, this can distort PPW and, hence, the PA. To understand the effect of wrist flexion, with all five subjects, readings were taken at three different values of wrist flexion namely $\theta = 30$ deg, 40 deg, and 50 deg, and the results are shown in Fig. 6(*b*). For all subjects, PA was found to be maximum when the angle was kept at 40 deg.

A similar pattern was observed in the shape of PPW with changing the angle of wrist extension (θ) as shown in Fig. 8. The shape of the waveform becomes irregular at $\theta = 30$ deg and 50 deg and is consistent at $\theta = 40$ deg, which coincides with maximum

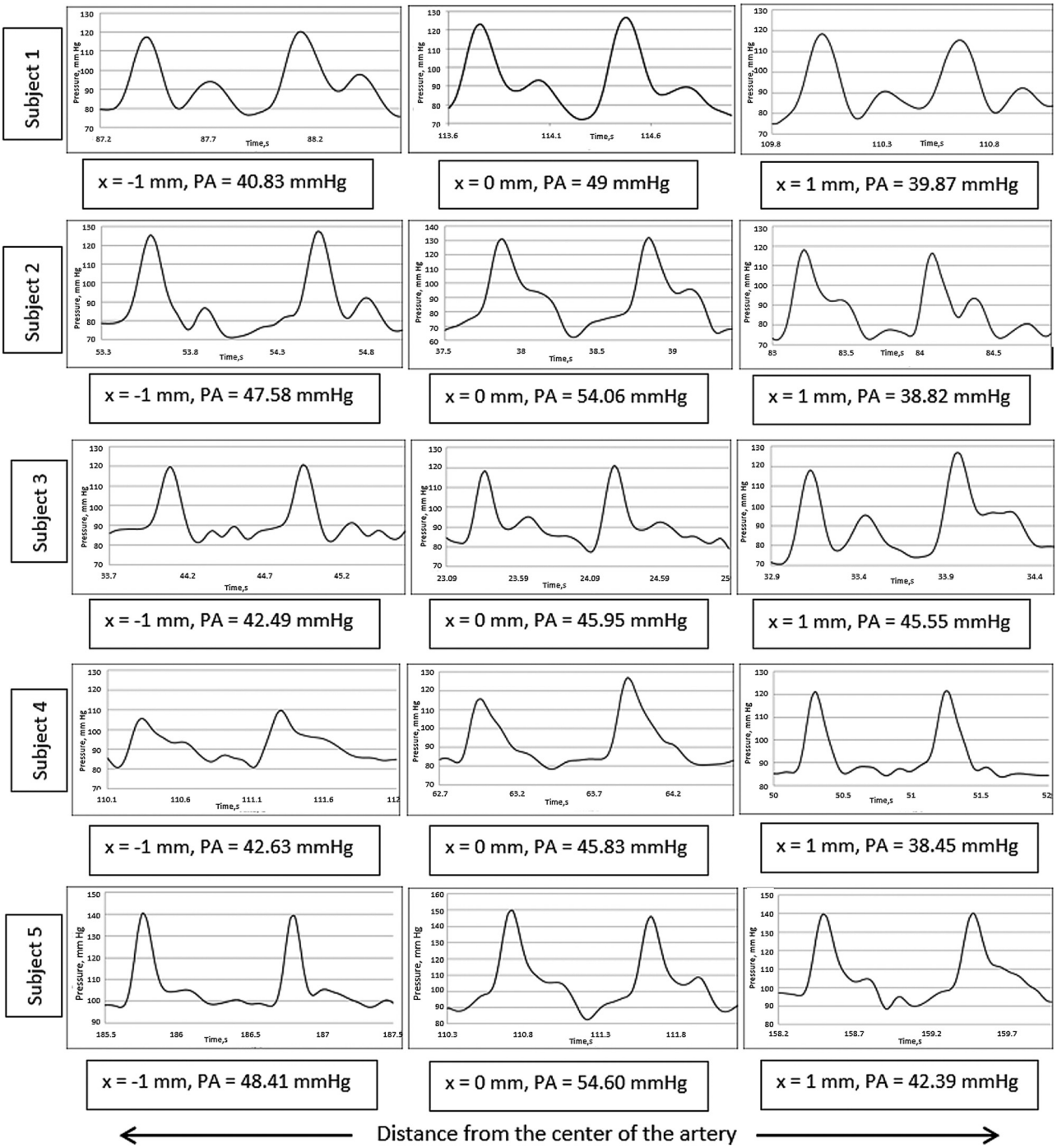

Fig. 7 Variation of PPW with the location of the gel head on the radial artery of five different subjects

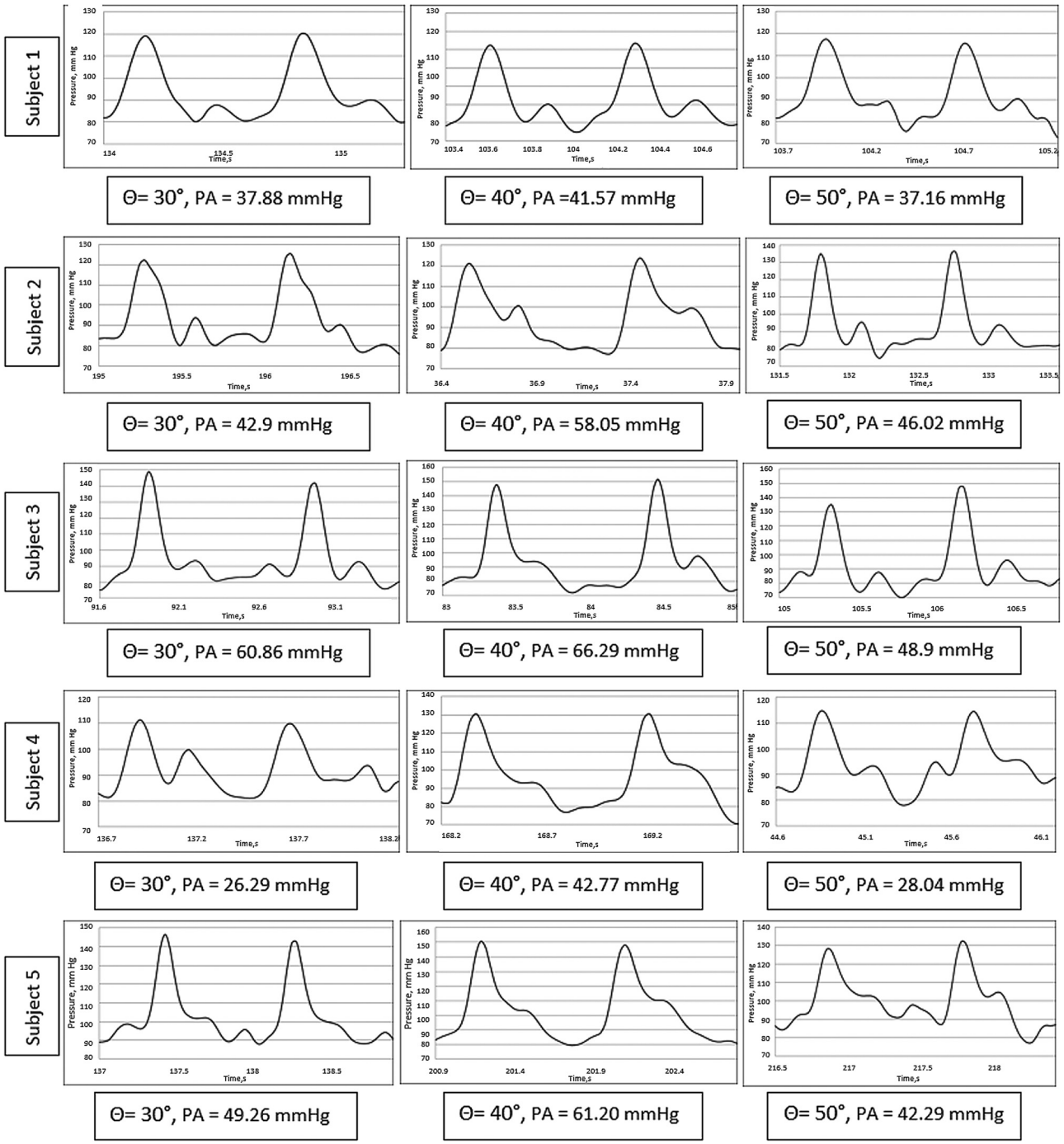

Fig. 8 Variation of PPW with the angle of extension of the wrist (Θ) for five different subjects

PA. At $\theta = 30$ deg the artery moves inside the tissue and is not easily accessible by the gel head, whereas at $\theta = 50$ deg, the artery is over-flattened, which causes an underestimated PA and a distorted PPW. For both angles, PPW becomes irregular due to improper contact between the gel head and the artery and hindered pressure transmission. It is clear that the PA changes as we change the angle of wrist extension for the subjects used here. An angle of 40 deg led to the most accurate representation.

4.5 Effect of Hold-Down Pressure. It is widely known that HDP is important in determining the shape of the PPW and the magnitude of PA. However, reaching the right HDP requires either user expertise or highly sensitive control systems. In the present device, the differential screw mechanism enables manual control of HDP in submillimeter steps. As shown in Fig. 9(*a*), on gradually increasing HDP by rotating the screw, PA first increases, reaches a maximum value, and then decreases. This trend is coherent with the literature [21–23]. The first peak in the figure (step 3) corresponds to average maximum PA for the loading steps, and the second peak (step 11) corresponds to average maximum PA during the unloading cycle. Ideally, the loading and unloading peaks should correspond to the same level of flattening and, hence, same PA. Here, the value was observed to be slightly higher during unloading. This may be attributed to the sudden increase in blood flow during the unloading steps of the artery, which may cause the first few waveforms to have higher amplitudes. This can be seen in Fig. 9(*c*) for the chosen unloading

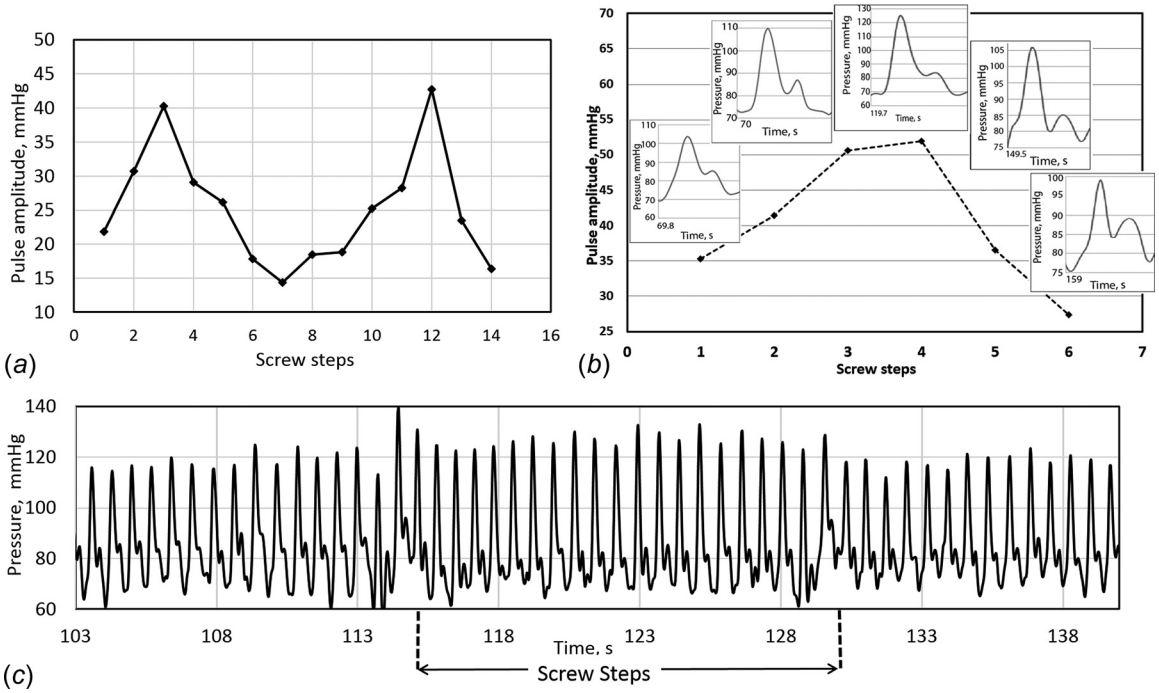

Fig. 9 (*a*) Variation of PA with the screw steps in a loading and unloading cycle, (*b*) variation of PPW with the screw steps during loading, and (*c*) calibrated PPW at the right hold down pressure

screw step. To account for this error, an improved data collection and postprocessing protocol should be incorporated in the future. Specifically, a longer data collection after each screw step will allow the artery and blood flow to stabilize for data recording for each step, and an improved algorithm will allow neglecting the first few waveforms immediately post screw rotation.

The shape of the waveform was also affected by HDP, shown in Fig. 9(*b*), for the loading steps. The waveforms were observed as regular and consistent when PA was maximum. This is expected since, as discussed in Sec. 3.1, maximum PA is observed when an artery is directionally unloaded in the vertical direction. Hence, at the level of compression corresponding to zero arterial wall stresses in the direction of loading, the gel head rides on top of the artery in all the pressure cycles, which results in the faithful transmission of forces acting due to blood pressure.

5 Limitations and Future Work

The device offers several improvements and modifications in the measurement of PPW via radial tonometry. One limitation of the device includes the need for user expertise, both in device centering via manual palpitation and in the application of HDP via manual screw rotation. Both these limitations will be addressed in future modifications via the use of feedback control for centering and a stepper motor for screw rotation. Another limitation of the device includes data validation and comparison using five healthy male subjects in the young age group (20 to 25 years). Cardiovascular disease arises later in life, and the incidence rate varies across age groups and sex of subjects. Future study will focus on increasing the number of subjects among different age groups, genders, and health conditions for validation of the device and for verification of other parameters used here such as the "flex-lock brace angle."

6 Summary and Conclusion

This paper presents design, development, and performance evaluation of a new modular tonometry device for measuring radial artery PPW. The device development and sensor pick-up design were guided by underlying computational analysis [25], which provided the basis for selection of optimum HDP. Maximum PA corresponding to zero arterial compliance was used as the indicator for the optimum level of arterial flattening to measure PPW. The pulse waveform collected as a function of percentage arterial flattening is one novel feature of the present device. Another feature includes patient-specific HDP for optimum amount of arterial flattening. A postprocessing algorithm allowed for right step identification for calculation of average PA for calibration to BP. Finally, the device was validated in a lab environment using limited subject data. The PPW measured was found to be sensitive to changes in operational parameters (gel-head placement, HDP, and wrist extension). Hence, a detailed protocol for data collection and analysis was also provided. Overall, the experiments showed a good correlation between the device and gold standard for both PA and PPW.

Since the device can be manufactured via a rapid fabrication technique, the current design provides a cost-effective solution for measuring PPW from the radial artery using a tactile-based force sensor. Future developments include device automation and optimization to improve user dependence and a clinical study for device validation.

Acknowledgment

Authors Mohammad Ikbal Choudhury, Rajneesh Juneja, Sitikantha Roy, and Anamika Prasad are co-applicants to an Indian patent (Provisional Patent Application No 201611027931) for the proposed new design discussed in the paper.

Funding Data

- Indo-US Grand Challenge Initiative-Affordable Blood Pressure Measurement Technologies for Low Resource Settings (Grant No IUSSTF/NIBIB_DST/ABPM/2013-2014/EOI_25.)

Nomenclature

BP = blood pressure
CI = confidence interval

FEA = finite element analysis
HDP = hold down pressure
MAP = mean arterial pressure
PA = pulse amplitude
PPW = pulse pressure waveforms
PWA = pulse waveform analysis
SD = standard deviation
TPT = total pulse duration Time

References

[1] Vierordt, K., 1855, *Die Lehre vom Arterienpuls in gesunden und kranken zustanden: gegründet auf eine neue Methode der bildlichen Darstellung des menschlichen Pulses*, Vieweg, Kranzberg, Germany, p. 22.

[2] Sesso, H. D., Stampfer, M. J., Rosner, B., Hennekens, C. H., Gaziano, J. M., Manson, J. E., and Glynn, R. J., 2000, "Systolic and Diastolic Blood Pressure, Pulse Pressure, and Mean Arterial Pressure as Predictors of Cardiovascular Disease Risk in Men," Hypertension, **36**(5), pp. 801–807.

[3] O'Rourke, M. F., Staessen, J. A., Vlachopoulos, C., Duprez, D., and Plante, G. E., 2002, "Clinical Applications of Arterial Stiffness; Definitions and Reference Values," Am. J. Hypertens., **15**(5), pp. 426–440.

[4] Kelly, R., and Fitchett, D., 1992, "Noninvasive Determination of Aortic Input Impedance and Outer Left Ventricular Power Output: A Validation and Repeatability Study of a New Technique," J. Am. Coll. Cardiol., **20**(4), pp. 952–963.

[5] Nakayama, Y., Tsumura, K., Yamashita, N., Yoshimaru, K., and Hayashi, T., 2000, "Pulsatility of Ascending Aortic Pressure Waveform is a Powerful Predictor of Restenosis After Percutaneous Transluminal Coronary Angioplasty," Circulation, **101**(5), pp. 470–472.

[6] O'Rourke, M., Pauca, A., and Jiang, X.-J., 2001, "Pulse Wave Analysis," Br. J. Clin. Pharmacol., **51**(6), pp. 507–522.

[7] Phillippe, F., Chemaly, E., Blacher, J., Mourad, J. J., Dibie, A., Larrazet, F., Laborde, F., and Safar, M. E., 2002, "Aortic Pulse Pressure and Extent of Coronary Artery Disease in Percutaneous Transluminal Coronary Angioplasty Candidates," Am. J. Hypertens., **15**(8), pp. 672–677.

[8] O'Rourke, M. F., 2009, "Time Domain Analysis of the Arterial Pulse in Clinical Medicine," Med. Biol. Eng. Comput., **47**, pp. 119–129.

[9] Chen, C.-Y., Wang, W.-K., Kao, T., Yu, B. C., and Chiang, B. C., 1993, "Spectral Analysis of Radial Pulse in Patients With Acute, Uncomplicated Myocardial Infarction," Jpn. Heart J., **34**(2), pp. 37–49.

[10] Tsuei, J., Cheng, C. H., Wang, Y. L., and Wang, W. K., 1996, "Pulse Spectrum Analysis of Hospital Patient With Possible Liver Problems," Am. J. Chin. Med., **14**(3–4), pp. 315–320.

[11] Hsu, T. L., Chao, P. T., Hsiu, H., Wang, W. K., Li, S. P., and Wang, Y. Y., 2006, "Organ-Specific Ligation-Induced Changes in Harmonic Components of the Pulse Spectrum and Regional Vasoconstrictor Selectivity in Wistar Rats," Exp. Physiol., **91**(1), pp. 163–170.

[12] Koen, M., and Pascal, V., 2002, "Development and Modeling of Arterial Applanation Tonometry: A Review," Technol. Health Care, **10**(1), pp. 65–76.

[13] Parka, C. M., Korolkovab, O., Daviesa, J. E., Parkerb, K. H., Siggersb, J. H., Marcha, K., Tillina, T., Chaturvedia, N., and Hughesa, A. D., 2014, "Arterial Pressure: Agreement Between a Brachial Cuff-Based Device and Radial Tonometry," J. Hypertens., **32**(4), pp. 865–872.

[14] Birch, A. A., and Morris, S. L., 2003, "Do the Finapres™ and Colin® Radial Artery Tonometer Measure the Same Blood Pressure Changes Following Deflation of Thigh Cuffs?," Physiological Meas., **24**(3), pp. 653–660.

[15] Nelson, M. R., Stepanek, J., Cevette, M., Covalciuc, M., Hurst, R. T., and Tajik, A. J., 2010, "Noninvasive Measurement of Central Vascular Pressures With Arterial Tonometry: Clinical Revival of the Pulse Pressure Waveform?," Mayo Clin. Proc., **85**(5), pp. 460–472.

[16] Lee, B., Jeong, J., Kim, J., Kim, B., and Chun, K., 2014, "Cantilever Arrayed Blood Pressure Sensor for Arterial Applanation Tonometry," IET Nanobiotechnol., **8**(1), pp. 37–43.

[17] Kim, E. G., Nam, K. C., Heo, H., and Huh, Y., 2009, "Development of an Arterial Tonometer Sensor," 31st Annual International Conference of the IEEE Engineering in Medicine and Biology Society (EMBS), Minneapolis, MN, Sept. 3–6, pp. 3771–3774.

[18] Shioya, K., and Dohi, T., 2013, "Blood Pressure Measurement Device Based on the Arterial Tonometry Method With Micro Triaxial Force Sensor," The 17th International Conference on Solid-State Sensors, Actuators and Microsystems (TRANSDUCERS & EUROSENSORS XXVII), Barcelona, Spain, June 16–20, pp. 2389–2392.

[19] Ng, K.-G., 2011, "Review of Measurement Methods and Clinical Validation Studies of Noninvasive Blood Pressure Monitors: Accuracy of Requirements and Protocol Considerations for Devices That Require Patient-Specific Calibration by a Secondary Method or Device before Use," Blood Pressure Monit., **16**(6), pp. 291–303.

[20] Tyan, C. C., Liu, S. H., Chen, J. Y., Chen, J. J., and Liang, W. M., 2008, "A Novel Noninvasive Measurement Technique for Analyzing the Pressure Pulse Waveform of the Radial Artery," IEEE Trans. Biomed. Eng., **55**(1), pp. 288–297.

[21] Driscoll, M. D., Arnold, J. M., and Sherebrin, M. H., 1995, "Applied Recording Force and Noninvasive Arterial Pulses," Clin. Invest. Med., **18**(5), pp. 370–379.

[22] Driscoll, M. D., Arnold, M. O., Marchiori, G. E., Harker, L. A., and Sherebrin, M. H., 1997, "Determination of Appropriate Recording Force for Noninvasive Measurement of Arterial Pressure Pulses," Clin. Sci., **92**(6), pp. 559–566.

[23] Yoon, Y. Z., Lee, M. H., and Soh, K. S., 2000, "Pulse Type Classification by Varying Contact Pressure," IEEE Eng. Med. Biol. Mag., **19**(6), pp. 106–110.

[24] Reddy, K. S., 2002, "Cardiovascular Diseases in the Developing Countries: Dimensions, Determinants, Dynamics and Directions for Public Health Action," Public Health Nutr., **5**(1A), pp. 231–237.

[25] Singh, P., Choudhury, I., Roy, S., and Prasad, A., 2016, "A Computational Study to Investigate Effect of Tonometer Geometry and Patient-Specific Variability on Radial Artery Tonometry," J. Biomech., **58**, pp. 105–113.

[26] Hollinger, A., and Wanderley, M. M., 2006, "Evaluation of Commercial Force-Sensing Resistors," International Conference on New Interfaces for Musical Expression (NIME), Paris, France.

[27] Baker, P. D., Westenskow, D. R., and Kuck, K., 1997, "Theoretical Analysis of Non-Invasive Maximum Pulse Amplitude Algorithm for Estimating Mean Blood Pressure," Med. Bio. Eng. Comput., **35**(3), pp. 271–278.

[28] Millasseau, S. C., Kelly, R. P., Ritter, J. M., and Chowenczyk, P. J., 2002, "Determination of Age-Related Increases in Large Artery Stiffness by Digital Pulse Contour Analysis," Clin. Sci., **103**(4), pp. 371–377.